

# Spatially Resolved Fast Swept Langmuir Probe Measurements in the Wendelstein 7-AS Stellarator

M. Schubert<sup>1</sup>, M. Hron<sup>2</sup>, M. Endler<sup>1</sup>, and W7-AS Team<sup>1</sup>

<sup>1</sup>*Max-Planck-Institut für Plasmaphysik, EURATOM Association, Garching, Germany*

<sup>2</sup>*Institute of Plasma Physics, EURATOM Association/IPP.CR, Academy  
of Sciences of the Czech Republic, Prague, Czech Republic*

## 1 Introduction

Langmuir probes are a common tool to measure fluctuations in the edge of a fusion plasma, because of their high spatial and temporal resolution. However, if one wants to know transport relevant quantities like fluctuations of the poloidal electric field or fluctuations of temperature (energy transport!), the generally applied technique, which is to measure floating potential  $U_{\text{fl}}$  and ion saturation current  $I_{\text{sat}}$  only, might contain too many simplifications. Particularly  $U_{\text{fl}}$  can only be related to the plasma potential  $U_{\text{pl}}$ , if one knows the actual electron temperature  $T_e$ .

$$U_{\text{pl}} = U_{\text{fl}} + \frac{k_{\text{B}} T_e}{e} \cdot \ln \left( (1 - \gamma_{\text{SE}}) \sqrt{\frac{m_i}{2\pi m_e} \frac{T_e}{T_e + T_i}} \right) \approx U_{\text{fl}} + 2.5 \cdot \frac{k_{\text{B}} T_e}{e}.$$

The factor 2.5 is valid in hydrogen plasmas without secondary electron emission from the probe tip ( $\gamma_{\text{SE}} = 0$ ), and with  $T_e = T_i$ . Additionally, if one wants to know energy transport, the fluctuations of the temperature and its phase relative to the electric field have to be taken into account.

$$\Gamma_{\text{LCFS}} = \frac{3}{2} k_{\text{B}} \left\langle n T \frac{-\nabla U_{\text{pl}} \times \vec{B}}{B^2} \right\rangle \cdot \vec{e}_r \approx \frac{3}{2} k_{\text{B}} \bar{T}_e \langle \tilde{n}_e \tilde{v}_r \rangle + \frac{3}{2} k_{\text{B}} \bar{n}_e \langle \tilde{T}_e \tilde{v}_r \rangle$$

where  $v_r$  is the radial  $\mathbf{E} \times \mathbf{B}$  velocity.

## 2 Diagnostic setup

The most promising way to obtain the desired  $\tilde{n}$ ,  $\tilde{T}_e$  and  $\tilde{U}_{\text{pl}}$  information with sufficiently high temporal and spatial resolution is to sweep the probe bias voltage and to deduce  $I_{\text{sat}}$ ,  $U_{\text{fl}}$  and  $T_e$  from the current-voltage characteristic. This method was applied before [1, 2] and, with a related approach, in [3]. In the earlier work, the sweep frequency of several 100 kHz was found to be marginal, since the amplitude of the fluctuations is still significant in this frequency range. We could further increase the sweep frequency and have for the first time extended the technique to a spatially resolving array of 15 Langmuir probe tips.

Temporal and spatial scales of turbulent structures in the edge of W7-AS are known to be of the order of 10  $\mu\text{s}$  and 1 cm perpendicular to the magnetic field [4]. To investigate the spatial structure of these fluctuations, the 15 cylindrical graphite tips are aligned

poloidally on one flux surface with 2 mm spacing between adjacent tips. The diameter of one tip is 1 mm and the effective collecting area  $A = 4 \text{ mm}^2$ . The array has been mounted on a fast reciprocating probe drive. The tips are biased and their voltage is swept by a common source, the design frequency for this sweep was chosen to be 1 MHz to achieve the required temporal resolution. Offset and sweep amplitude of the applied voltage are chosen such that it stays below floating potential, and the stationary sheath characteristic

$$I = A \frac{n}{2} \left( c_s - \frac{\bar{c}_e}{2} \exp \left( \frac{e(U - U_{pl})}{k_B T_e} \right) \right)$$

is assumed to be valid, where  $c_s$  is the ion sound velocity and  $\bar{c}_e$  is the mean thermal velocity of the electrons. Individual currents are measured as a voltage drop across shunt resistors, placed between the source and every tip. Since the current measurement needs to be in the ‘hot’ branch of the circuit, the differential amplifiers must be able to handle both high voltage and high common mode. A strong miniaturization and high bandwidth are features of the amplifier design [2].

### 3 Calculation of plasma quantities

The primary data are  $U(t)$  and  $I_i(t)$  traces containing the current response of tip  $i$  to the common voltage  $U$ . In these traces, individual characteristics have to be addressed. This is done by finding the corresponding and dominating maxima of the first harmonic of the sweep and cutting the data in between these maxima into packets, each containing a single or several sweep periods. The characteristics usually have a slight phase shift between current and voltage, leading to a systematic difference of fitted floating potential and temperature between up and down part of the sweep. A smooth evolution of quantities without a systematic difference can be obtained by optimizing the phase shift. Particularly the floating potential has been observed to be most sensitive to this.

The output of the fitting routine processing the single characteristics are  $I_{\text{sat}}$ ,  $U_{\text{fl}}$  and  $T_e$  together with their uncertainties [5]. In contrast to a direct measurement of  $I_{\text{sat}}$  and  $U_{\text{fl}}$ , each sample of these quantities is only the output of the fit and, since the fit does not necessarily converge, it is possible that gaps appear in the result. A post-processing routine identifies these gaps by looking for either a fit fail or a large uncertainty of the fit parameter. The gaps are interpolated, using the nearest successful previous and next fits that have a small uncertainty.

A first step validation of the fitted quantity  $U_{\text{fl}}$  was done by calculating the cross correlation between a swept and an adjacent stationary floating probe and comparing to the cross correlation between two floating probes. This showed satisfactory agreement.

### 4 Analysis of fluctuating quantities

After creating the time traces of the primary fit parameters  $I_{\text{sat}}$ ,  $U_{\text{fl}}$  and  $T_e$ , we have, as a first step in the analysis of the fluctuations of these quantities, calculated the poloidal-temporal (auto-)correlation functions. Results for a location  $1.5 \pm 0.5 \text{ cm}$  outside the last

closed magnetic surface are displayed in the figure. In this case, the quantities display a very similar structure, which agrees for the cases of  $\tilde{I}_{\text{sat}}$  and  $\tilde{U}_{\text{fl}}$  with previous stationary (non-swept) measurements. We can in our example read a lifetime of  $\sim 30 \mu\text{s}$ , a poloidal scale length of  $\sim 2.5 \text{ cm}$  and poloidal velocities of  $650 \text{ m/s}$  ( $I_{\text{sat}}$ ),  $450 \text{ m/s}$  ( $U_{\text{fl}}$ ) and  $800 \text{ m/s}$  ( $T_e$ ) from these figures. The poloidal velocity of the structures is caused mainly by the  $E \times B$  velocity due to the radial electric field. As this is positive (directed radially outwards) in the SOL of W7-AS, the propagation of the main feature of the correlation function is in the direction of the ion diamagnetic drift. In the case of  $U_{\text{fl}}$ , a second and smaller component, propagating in the opposite direction with  $\sim 3000 \text{ m/s}$  is visible.

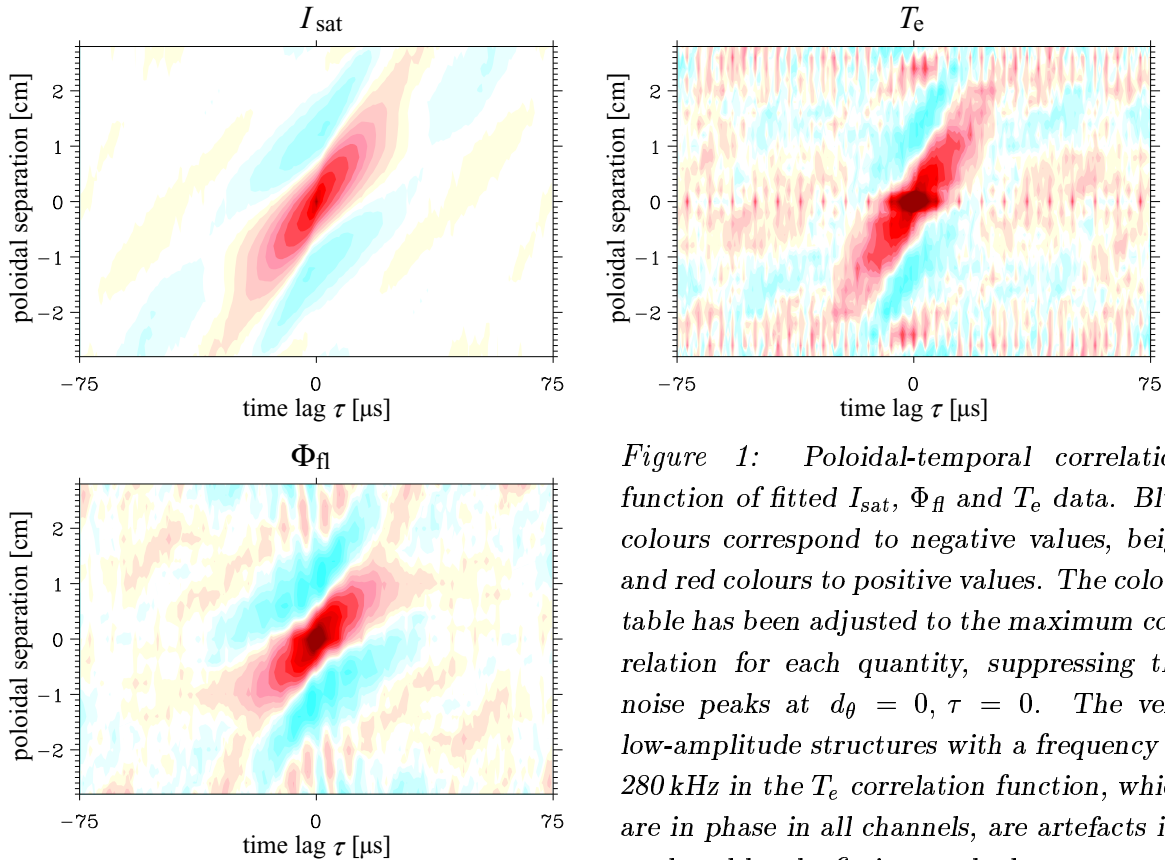


*Figure 1: Poloidal-temporal correlation function of fitted  $I_{\text{sat}}$ ,  $\Phi_{\text{fl}}$  and  $T_e$  data. Blue colours correspond to negative values, beige and red colours to positive values. The colour table has been adjusted to the maximum correlation for each quantity, suppressing the noise peaks at  $d_{\theta} = 0$ ,  $\tau = 0$ . The very low-amplitude structures with a frequency of  $280 \text{ kHz}$  in the  $T_e$  correlation function, which are in phase in all channels, are artefacts introduced by the fitting method.*

## 5 Discussion

The characteristic of the sheath is valid, as long as the sweep frequency stays far below the ion plasma frequency [6]. However, a phase shift between voltage and current may appear at high frequencies because the flux tube beyond the sheath is not an ideal conductor for the probe current flowing mainly along a field line. The electrical properties of the flux tube can be described by a complex impedance, the main components of which are polarization currents [7], parallel and perpendicular conductivity [8] and vacuum inductance. The plasma in front of the probe tip has then similar electric properties as a coaxial cable [9]. It would be attractive to use the impedance as an additional fit parameter during evaluation of the characteristic, because it contains information about

plasma quantities in the flux tube. However, this involves numerical difficulties, since the shift is comparatively small ( $\sim \pi/10$  at  $f_{\text{sweep}} = 1$  MHz) and the additional fit parameters introduced render the fitting problem ill-posed. For the analysis used here, a fixed phase shift has been used instead, which was optimized as described in section 3.

The observation of slightly different poloidal velocities for the different plasma quantities cannot yet be generalised, but a larger database under different discharge conditions and for different radial positions in the plasma edge must be analysed.

## 6 Conclusion and Outlook

We have demonstrated that it is possible to obtain simultaneous and spatially highly resolved information on the structure of  $I_{\text{sat}}$ ,  $U_{\text{fl}}$  and  $T_e$  fluctuations in the SOL of a fusion experiment by applying a high-frequency sweep voltage to a multi-tip Langmuir probe array.

The fitting procedure applied so far for obtaining the fluctuating plasma quantities from the current-voltage characteristics introduces some amount of high-frequency noise into the calculated quantities, leaving still possibilities for optimization, and an improved fit model might even allow to determine further information on the plasma in front of the swept probe tips.

The next step in our analysis will be the investigation of the cross correlation between  $\tilde{I}_{\text{sat}}$ ,  $\tilde{U}_{\text{fl}}$  and  $\tilde{T}_e$ , where in particular the relative phase between them is of interest for the comparison with theory and numerical simulations and for the reliable calculation of the radial particle and heat transport.

- [1] R. Balbín et al., Rev. Sci. Instrum. **63** (1992) 4605;  
C. Hidalgo et al., Phys. Rev. Lett. **69** (1992) 1205;  
L. Giannone et al., Phys. Plasmas **1** (1994) 3614.
- [2] U. Pfeiffer et al., Contrib. Plasma Phys. **38** (1998) 134.
- [3] M. A. Meier et al., Rev. Sci. Instrum. **66** (1995) 437; M. A. Meier et al., Contrib. Plasma Phys. **38** (1998) 98.
- [4] M. Endler et al., Physica Scripta **51** (1995) 610.
- [5] Numerical Algorithms Group, Fortran Library Manual, Mark 19, Chapter E04 (1999).
- [6] P. Verplancke, PhD thesis, University of Ghent, IPP report 4/275 (1997).
- [7] A. V. Nedospasov and D. A. Uzdensky, Contrib. Plasma Phys. **34** (1994) 478.
- [8] M. Weinlich, PhD thesis (in German), IPP report 5/64 (1995).
- [9] A. Geier and H. Niedermeyer, Contrib. Plasma Phys. **38** (1998) 86.